Distributed Entrainment Sink Approach for Modeling Mixing and Transport in the Intermediate Field

K. W. Choi[1] and Joseph H. W. Lee[2]

Abstract: In densely populated coastal cities in Asia, wastewater outfalls are often located not far from sensitive areas such as beaches or shellfisheries. The impact and risk assessment of effluent discharges poses particular technical challenges, as pollutant concentration needs to be accurately predicted both in the near field and intermediate field. The active mixing close to the discharge can be modeled by proven plume models, while the fate and transport far beyond the mixing zone can be well-predicted by three-dimensional (3D) circulation models based on the hydrostatic pressure approximation. These models are usually applied separately with essentially one-way coupling; the action of the plume mixing on the external flow is neglected. Important phenomena such as surface buoyant spread or source-induced changes in ambient stratification cannot be satisfactorily addressed by such an approach. A Distributed Entrainment Sink Approach is proposed to model effluent mixing and transport in the intermediate field by dynamic coupling of a 3D far field shallow water circulation model with a Lagrangian near-field plume model. The action of the plume on the surrounding flow is modeled by a distribution of sinks along the plume trajectory and an equivalent diluted source flow at the predicted terminal height of rise. In this way, a two-way dynamic link can be established at grid cell level between the near and far-field models. The method is demonstrated for a number of complex flows including the interaction of a confined rising plume with ambient stratification, and the mixing of a line plume in cross flow. Numerical predictions are in excellent agreement with basic laboratory data. The general method can be readily incorporated in existing circulation models to yield accurate predictions of mixing and transport in the intermediate/far field.

DOI: 10.1061/(ASCE)0733-9429(2007)133:7(804)

CE Database subject headings: Plumes; Coupling; Environmental impacts; Urban areas; Asia; Fish management.

Introduction

For environmental risk assessment it is necessary to predict the impact of effluent discharges for a wide range of discharge and ambient conditions. For many densely populated coastal cities in Asian Pacific countries, this prediction poses particular technical challenges. The effluent discharges are often located in relatively shallow waters of 5–20 m depth, not far (e.g., 5–10 km) from sensitive receivers such as beaches and fisheries. Sound management decisions on the appropriate degree of treatment must be based on impact assessment models that can cater to both the near field and intermediate/far field.

In the vicinity of the discharge ("near field"), the buoyant jet trajectory and mixing can be well-predicted by a validated integral model that predicts the turbulent entrainment as a function of source characteristics, ambient velocity, and stratification (Fig. 1). Near field models can resolve down to scales of the order of the jet diameter; typical time and length scales of the plume rise are in the order of minutes and water depths, respectively. On the other hand, in the "far field," the effluent is passively transported by ambient currents and further diluted by turbulent diffusion; typical time and length scales are on the order of hours and kilometers. In the near-far field transition ("intermediate field"), the dynamics depends on the interaction of the near-field plume mixing and the ambient flow, which can result in changes in background concentration, gravitational spreading, and modifications in ambient stratification. These phenomena have been observed and documented in laboratory studies (e.g., Baines and Turner 1969; Wallace and Wright 1984; Lee and Cheung 1986; Wong 1986; Roberts 1979). However, the numerical prediction of such flows has hitherto not been reported.

The large disparity of time and length scales in the near and far fields is well known, and effluent mixing and transport beyond the near field has been explored in several studies. As an extreme case, the effluent buoyant jet is modeled as a freshwater source in a single grid cell in the far-field model (Blumberg et al. 1996). The plume trap height and dilution is computed as a function of ambient velocity and density profile derived from the far-field model. Zhang and Adams (1999) studied near-far field coupling by employing the three-dimensional (3D) circulation model ECOMsi and the near-field model RSB. Four methods for interfacing the near and far-field models were considered: (1) introduce the discharge flow and pollution load (tracer mass flux) as source terms at the discharge point; (2) introduce source flow at discharge point, and release the pollution load at the trap height predicted by RSB; (3) introduce both the diluted flow and the pollution load at the predicted trap height; and (4) only introduce the pollution load at the predicted trap height. The last method is the most commonly adopted approach in practice. As the near-field model RSB provides only a predicted plume trap height,

[1]Postdoctoral Fellow, Dept. of Civil Engineering, The Univ. of Hong Kong, Pokfulam Road, Hong Kong. E-mail: choidkw@hkucc.hku.hk

[2]Professor, Dept. of Civil Engineering, The Univ. of Hong Kong, Pokfulam Road, Hong Kong. E-mail: hreclhw@hkucc.hku.hk

Note. Discussion open until December 1, 2007. Separate discussions must be submitted for individual papers. To extend the closing date by one month, a written request must be filed with the ASCE Managing Editor. The manuscript for this paper was submitted for review and possible publication on September 27, 2005; approved on December 28, 2006. This paper is part of the ***Journal of Hydraulic Engineering***, Vol. 133, No. 7, July 1, 2007. ©ASCE, ISSN 0733-9429/2007/7-804–815/ $25.00.

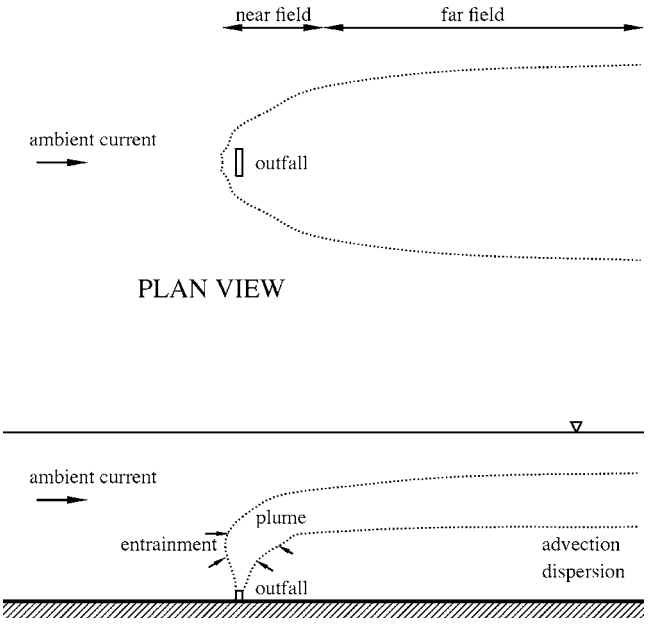

Fig. 1. Mixing and transport of effluent discharge

dilution, and width for each ambient condition, the interaction of the near-field mixing with the ambient flow cannot be accounted for by this approach. In addition, the correct reproduction of plume trap height and dilution is dependent on grid resolution, and the parametrization of the horizontal and vertical diffusivities (Zhang and Adams 1999). More important, these near-far field coupling methods have not been validated against experimental data.

Kim et al. (2002) coupled a jet integral model with a particle tracking model to simulate the mixing of a single buoyant jet discharge. Far-field mixing and transport are simulated by particles introduced at the equilibrium rise height or the end of the computed initial mixing zone. The model results were compared with laboratory experiments for a nonstratified cross flow. The flow field or velocity distribution was not generated by 3D flow model, but interpolated from the integral jet model predictions. Although the two models are linked, there is negligible dynamic interaction between them. More recently, Bleninger and Jirka (2004) proposed a methodology to couple the near-field CORMIX model and the Delft3D circulation model. An approach similar to Method 3 of Zhang and Adams (1999) is adopted, whereby the discharge volume and mass fluxes at the terminal height computed by CORMIX are incorporated into the far-field model.

All of the above-mentioned methods involve either "one-way coupling" or weakly "two-way coupling"; hence the dynamic effects of the plume mixing are not satisfactorily represented in the far-field model. The interpretation of experimental data is also hampered by the lack of a general robust numerical prediction method for mixing in the intermediate field. For example, outfall diffuser design is often based on semiempirical correlations of laboratory data of plane buoyant jets in linearly stratified fluid (Wallace and Wright 1984; Lee and Cheung 1986; Jirka and Lee 1994). Nevertheless, as the ambient stratification in the finite laboratory flume undergoes continuous modification by the introduction of the jet discharge, the effect of the limited flume length and changing ambient density on the results has yet to be clarified. Further, near-field plume models are valid only up to the base of the spreading layer. In many situations, a theoretical prediction of initial dilution necessitates a meaningful coupling of the vertical plume rise region with the horizontal buoyant spreading layer in the intermediate field. For example, Koh (1983) used an analytical model to show the upper layer thickness of a line plume in stagnant uniform fluid to be about 30% of the depth.

In this paper, we present a general Distributed Entrainment Sink Approach (DESA) for the effective modeling of mixing and transport in the intermediate field. The near-field mixing is modeled by a Lagrangian plume model (JETLAG, Lee and Cheung 1990; Lee and Chu 2003), while the far-field transport is simulated by the Environmental Fluid Dynamics Code (EFDC, Hamrick 1992). It is shown that the near-field mixing can be satisfactorily represented in the far-field model by embedding the near-field predictions at "grid cell" level. The accuracy of the method is demonstrated by comparing the numerical model predictions with experimental data in representative laboratory experiments of prototype environmental transport problems.

Method of Dynamic Coupling

All the previous approaches of near-far field coupling provide essentially only one-way coupling; the active mixing induced by the buoyant effluent discharge is not fully represented in the far-field model. From the viewpoint of the surrounding water, the important near-field flows are the bulk sink flows ("loss") due to the turbulent jet entrainment and the bulk source flows ("gain") due to the diluted discharges (mixed effluent). In order to have a true two-way coupling, it is proposed to represent the discharge by introducing in the far-field model: (1) a series of entrainment sinks along the predicted plume trajectory; and (2) the diluted source flow and pollution loading at the predicted terminal level of plume rise. The sources and sinks are determined from a near-field model embedded within the far-field model.

The key difference between this new method (DESA) and the commonly employed "source only" methods is that the near-field mixing is fully resolved by the subgrid plume model; the bulk fluid and tracer mass transport induced by the effluent discharge as well as the influence of background concentrations or recirculation on the near field can be fully modeled in a dynamic manner. It ensures mass conservation in the system and models the interaction of plume entrainment and ambient flow in a way similar to the "filling box" mechanism described by Turner (1973). The mixed effluent flow, which is usually at least one to two orders of magnitude greater than the discharge flow, and mass sources fill up the spreading layer at the terminal level, whereas the entrainment sinks draw the ambient fluids back into the plume. This interaction of the plume and the surrounding flow induces additional mixing beyond the near field. The effect of unsteady evolution of the ambient flow on the plume trajectory and dilution, as well as the changes in plume mixing on the ambient flow are fully accounted for.

Near-Field Mixing

The Lagrangian model JETLAG (Lee and Cheung 1990; Lee and Chu 2003) is employed for plume modeling in the near field. JETLAG is a well-proven robust jet model that predicts the mixing of an arbitrarily inclined round buoyant jet in a stratified cross flow, with a 3D trajectory. It tracks the evolution of the average properties of a plume element by conservation of horizontal and vertical momentum, conservation of mass accounting for shear and vortex entrainment, and conservation of solute or tracer mass/heat. For a given set of ambient conditions (vertical profile of

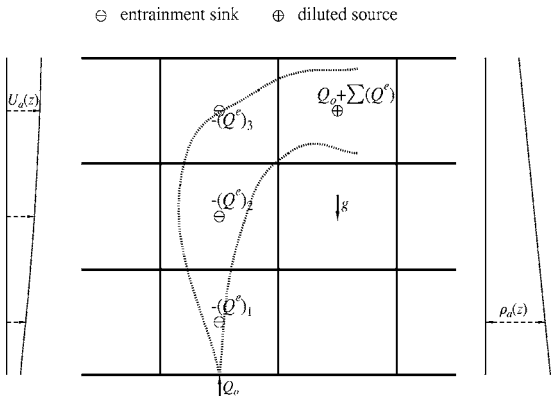

Fig. 2. Representation of plume mixing by diluted source flow and entrainment sinks along the jet trajectory

horizontal velocity, density, and tracer concentration), the jet trajectory, jet velocity and radius, and dilution (entrainment) can be predicted. The turbulent entrainment along the jet trajectory can then be obtained from the discharge point up to a terminal level (free surface, bottom, or trap level in the presence of ambient density stratification). The boundary conditions for the near-field model depend on the external (intermediate or far field) flow, which can be obtained from a 3D circulation model.

The effect of the near-field mixing on the intermediate-field flow can then be represented as follows (Fig. 2). The plume mixing is represented as a series of distributed sinks along the jet trajectory. Also, a source term representing the diluted source (total dilution) flow and the discharged pollution loading (tracer mass flux) is introduced at the terminal level. These volumetric and mass source/sinks are introduced into the governing transport equations for the 3D circulation model (see later discussion). We have the continuity equation as

$$\frac{\partial U}{\partial x}+\frac{\partial V}{\partial y}+\frac{\partial W}{\partial z}=Q_s \tag{1}$$

and the solute mass transport equation (for both salinity and tracer) as

$$\frac{\partial(HC)}{\partial t}+\bar{\nabla}\cdot\nabla(HC)=\frac{\partial}{\partial x}\left[HA_H\frac{\partial C}{\partial x}\right]+\frac{\partial}{\partial y}\left[HA_H\frac{\partial C}{\partial y}\right]+\frac{\partial}{\partial z}\left[K_H H\frac{\partial C}{\partial z}\right]+Q_c \tag{2}$$

where U, V, and W=turbulent-mean velocity components in the x-, y-, z-directions, respectively; $\bar{\nabla}\cdot\nabla(\,)\equiv U\partial(\,)/\partial x+V\partial(\,)/\partial y+W\partial(\,)/\partial z$; H=water depth; C=solute concentration; A_H=horizontal eddy diffusivity; K_H=vertical eddy diffusivity; Q_s=volumetric source/sink term representing the entrainment or diluted flows; and Q_c=source/sink term for the solute or tracer mass. Both of these terms can be obtained at "grid cell" level from the near-field model, and account for the fluid volume flux and buoyancy changes. By the nature of the hydrostatic approximation of the circulation model, the jet momentum is not explicitly included as source terms in the momentum equations; rather its effect is introduced via the jet entrainment computed by the Lagrangian plume model.

As the ambient conditions provided by the far-field model (vertical profile of upstream velocity, solute concentration, and density) change, the near-field plume behavior changes correspondingly. The changes in jet trajectory and dilution will be reflected in the positions and strengths of the sources and sinks.

Intermediate/Far-Field Transport

In the present study, the 3D flow model is based on the Environmental Fluid Dynamics Code (EFDC) for solving free surface flow and transport problems (Hamrick 1992). EFDC is a finite difference model that solves the shallow water equations using the Mellor and Yamada (1982) scheme for turbulent closure. The system of governing equations including the continuity, momentum, and transport equations provides a closed system for the variables U, V, W, P, η, ρ, S, and T, where ρ=fluid density; S=salinity; T=temperature; and η=free surface level above a reference datum. The pressure P is assumed to be hydrostatic and consists of barotropic (induced by external free surface gravity) and baroclinic (induced by the horizontal density gradient) components. The model uses a staggered grid for discretization and a sigma-grid coordinate in vertical direction. The modal splitting technique is used to solve the discretized equations.

The horizontal turbulent diffusivity is given by

$$A_H=C\Delta x\Delta y\left[\left(\frac{\partial U}{\partial x}\right)^2+\frac{1}{2}\left(\frac{\partial V}{\partial x}+\frac{\partial U}{\partial y}\right)^2+\left(\frac{\partial V}{\partial y}\right)^2\right]^{1/2} \tag{3}$$

where C=Smagorinsky coefficient has a value in the range of C=0.1–0.2. For the present study, C=0.17 is adopted based on model comparison against experimental data of salinity intrusion in a laboratory tidal flume (Thatcher and Harleman 1972; Choi 2002). An advantage of the Smagorinsky relation is that A_H decreases with improved grid resolution and decreasing velocity gradients, thus avoiding the introduction of excessive horizontal dispersion.

Based on the second moment turbulence closure model developed by Mellor and Yamada (1982), the vertical turbulent viscosity and diffusivity can be related to the turbulent kinetic energy, $q^2/2$, a turbulence length scale, l, and a "turbulent" Richardson number

$$\mathrm{Ri}_q=-\frac{gl^2}{q^2}\left(\frac{1}{\rho_0}\frac{\partial\rho}{\partial z}\right).$$

$q^2/2$ and l are determined by a pair of transport equations; the standard turbulence model constants for the EFDC model are adopted (Hamrick 1996).

After introducing the plume-induced source/sink terms, the governing equations of the 3D circulation model [Eq. (1) for fluid mass, Eq. (2) for each tracer mass, plus the fluid momentum and turbulent transport equations] can be solved to yield the updated flow and scalar fields. With the computed flow and solute/tracer mass distributions in the far field, the near-field plume model can then be driven by the updated ambient conditions to generate the new source and sink terms for the next time step. The coupling of the models is summarized by the flow chart shown in Fig. 3. Any changes in one model will immediately be passed to the other model; a two-way dynamic coupling between the near and far-field models is ensured.

Details of Near-Far Field Coupling

In the Lagrangian model JETLAG, the position and average properties of a plume element is tracked (Lee and Cheung 1990; Lee and Chu 2003). The turbulent mass entrainment into a plume element, ΔM_p, consists of: (1) the shear entrainment computed as

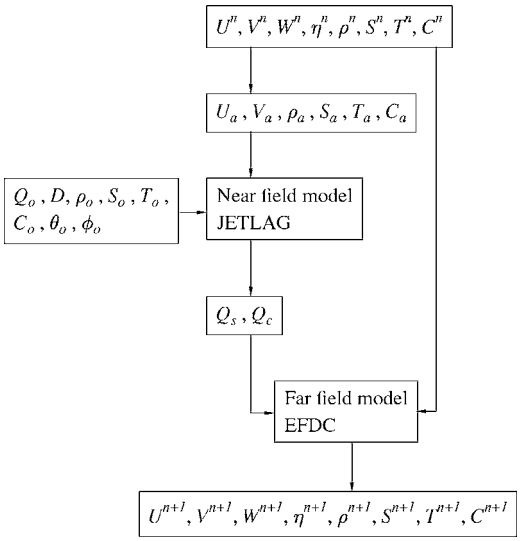

Fig. 3. Schematic flow chart for dynamic coupling between near- and far-field models

a function of the relative jet velocity in the direction of the jet axis, the radius and the thickness of the plume element; and (2) the vortex entrainment due to the ambient cross flow, which is a function of the ambient density and velocity, the radius and the thickness of the plume element, and the inclination of the plume element with respect to the ambient current [Figs. 4(a and b)]. In model implementation, the entrainment flow into each plume element is assigned to the corresponding far-field model grid cell based on the location of the center of the computed plume elements [Figs. 4(b and c)]. The entrainment sink for each far-field model grid cell (Q_s^e) can then be computed by summing up all the entrainment flows assigned to it, i.e.

$$Q_s = -Q_s^e = -\sum \left(\frac{\Delta M_p}{\rho_a \Delta t} \right) \tag{4}$$

and the corresponding tracer mass flux (Q_c^e) similarly computed as

$$Q_c = -Q_c^e = -Q_s^e C_a \tag{5}$$

where ρ_a and C_a=ambient density and solute concentration, respectively, determined from the values of the eight neighboring grid cells [Fig. 4(c)].

The diluted source flow (Q_s^d) and the corresponding tracer mass flux (Q_c^d) at the terminal level are then computed by summing the effluent and all the entrainment flows, i.e.

$$Q_s^d = Q_0 + \sum Q_s^e \tag{6}$$

and

$$Q_c^d = Q_0 C_0 + \sum Q_c^e \tag{7}$$

where Q_0, C_0 are the effluent discharge flow and tracer concentration, respectively. The dilution flow is applied as a source term to the circulation model grid cell that contains the center of the plume element at the terminal level. Computing the diluted source flow in this way ensures mass conservation, as the additional dilution flow is canceled out by the negative entrainment flow.

The advantages of the proposed approach over previous "source only" methods can be summarized as follows: (1) it fully accounts for the entrainment and dilution, hence the induced mixing, due to the buoyant discharge in the far-field circulation model; (2) the complete 3D jet trajectory is represented instead of just a single discharge point; (3) the use of the Lagrangian plume model enables the near-field simulation to be carried out independent of the circulation model grid; and (4) with a validated near-field plume model, the DESA method can be applied to all types of buoyant discharges without the need for fine-tuning the circulation model parameters.

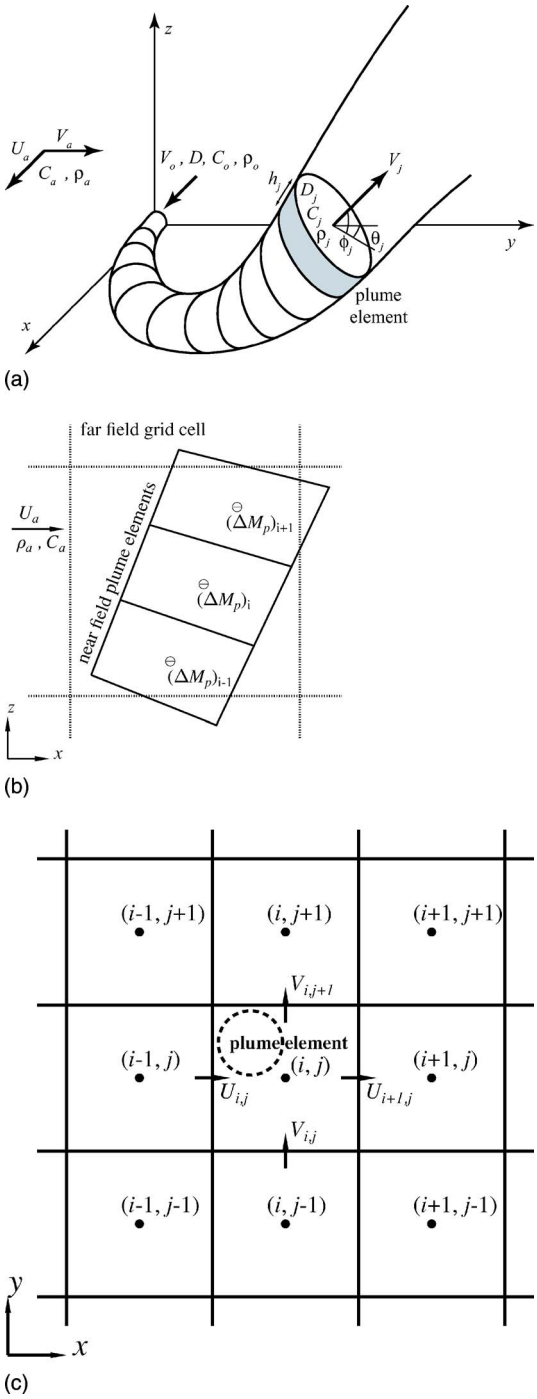

Fig. 4. (a) 3D jet trajectory predicted by Lagrangian near-field model; (b) near-field mixing representation in far-field grid cell; and (c) ambient velocity and concentration determined by the far-field model.

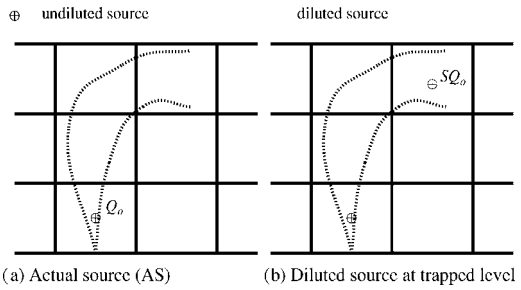

Fig. 5. Alternative representation of near-field mixing by "source-only" methods (S=average dilution)

Comparison of Numerical Model Prediction with Data

The application of the proposed dynamic near-far field coupling is illustrated for several representative mixing and transport problems—ranging from round and plane buoyant jets in stratified fluid, to line plumes in stratified cross flow. The predictions of the coupled model are compared with basic laboratory data. As the reference for assessing the performance of the proposed method, three alternative "source only" methods are also considered:

1. Undiluted source introduced at discharge point [Actual Source (AS)]: It is a commonly used approach in engineering practice when only the far-field model is used. The volumetric and mass source terms are introduced at the discharge point in the continuity and mass transport equations [Fig. 5(a)].
2. Diluted source and mass source terms introduced at the terminal level determined by the embedded near-field model [Diluted Source at Trapped Level (DSTL)] [Fig. 5(b)]: This method (Approach 3 in Zhang and Adams 1999) does not account for the entrainment action on the far-field flow. The near-field model is driven by the updated ambient conditions from the far-field model, while the location and strength of the source terms in the far-field model are updated by the near-field model.
3. Undiluted source included at the location determined by the embedded near-field model [Undiluted Source at Trapped Level (USTL)]: It is similar to DSTL except that the undiluted source is applied to ensure exact water mass conservation.

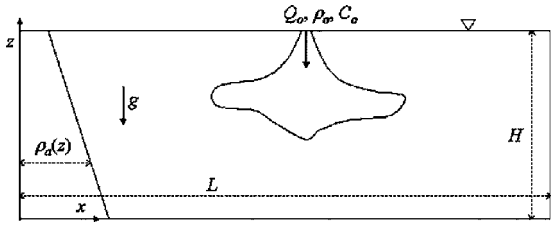

Fig. 6. Vertical round buoyant jet in stagnant linearly density-stratified ambient fluid

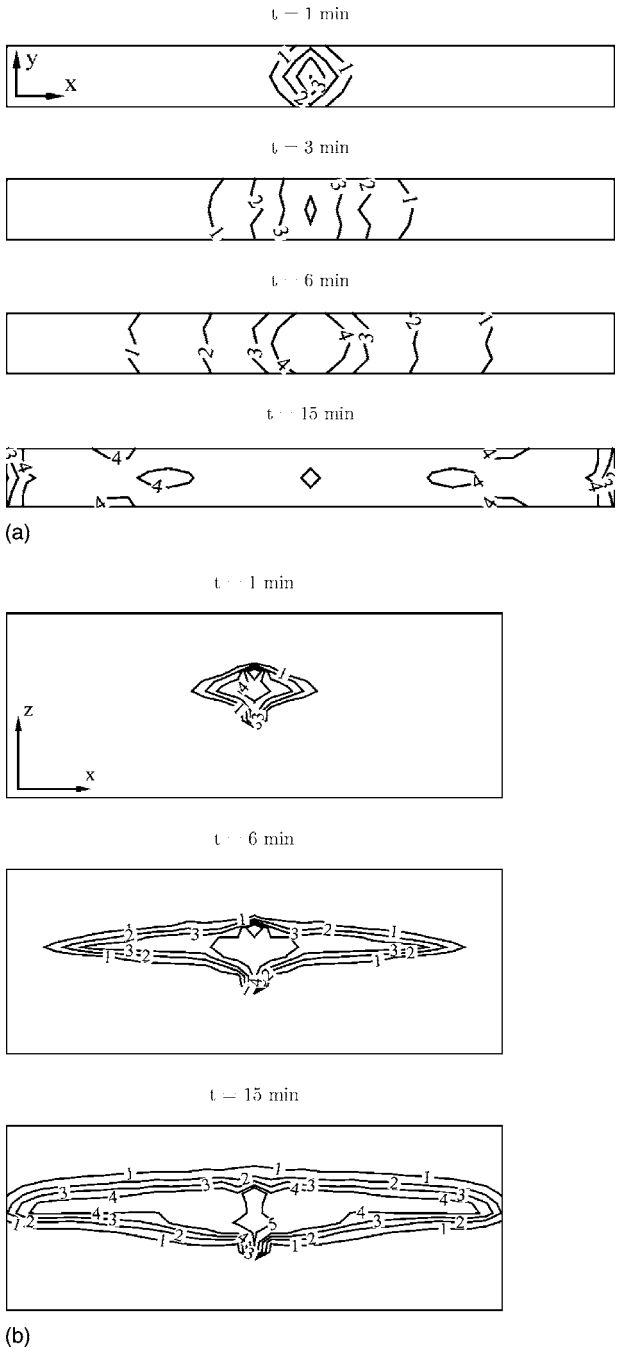

Fig. 7. Computed tracer concentration distribution (in $0.01C_0$ units) (a) in the horizontal plane (at trapping level) for a vertical round buoyant jet in stratified ambient at selected times; (b) in the vertical section (through the discharge point) for a round buoyant jet in stratified ambient

Test Case 1: Vertical Round Buoyant Jet in Stagnant Linearly Density-Stratified Ambient Fluid

The interaction between a buoyant jet and the ambient fluid can be illustrated for a round jet in otherwise stagnant linearly stratified fluid. The numerical prediction using the present method is compared with a well-documented experiment by Wong (1986). In his experiment, the (negatively) buoyant jet was created by discharging saline fluid downward from a circular orifice into a linearly stratified receiving water in a 457 cm×61 cm×91 cm deep tank (Fig. 6). Figs. 7–9 show the numerical predictions for

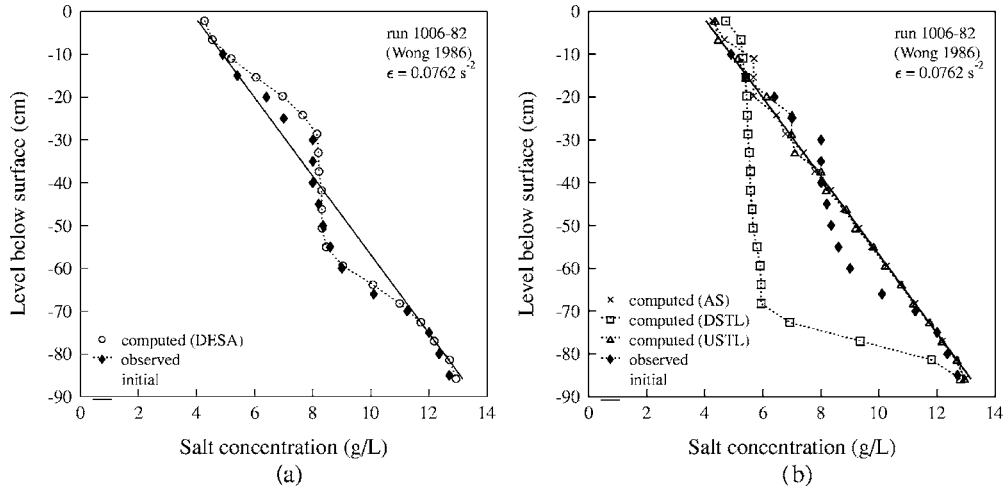

Fig. 8. Ambient salt concentration profiles before and after a round jet discharge into a linearly stratified fluid [observed data are adapted from Fig. 4.2.6 of Wong (1986)] by: (a) DESA method; (b) alternative "source-only" methods

an experiment with a vertical momentum-dominated buoyant jet in linearly stratified fluid (Run 1006-82, Wong 1986). The key experimental parameters are: $D=0.511$ cm; $V_0=1.518$ m/s; source densimetric Froude number $\mathrm{F}=V_0/\sqrt{gD(\rho_0-\rho_a(0))/\rho_a(0)}=112$, where $\rho_a(0)$=ambient density at source level; and ambient stratification parameter $\varepsilon=-[g/\rho_a(0)](d\rho_a/dz)=0.0762$ s^{-2}.

A $21\times3\times20$ model grid (with $\Delta x=21.8$ cm by $\Delta y=20.3$ cm and 20 uniform vertical layers) closed at the four sides is employed. The model is cold started and run for a duration of 15 min, similar to the length of experiment. A time step not greater than 0.25 s (with maximum Courant number $\mathrm{Cr}=\sqrt{gH}\Delta t/\Delta x\approx3.7$ and $u\Delta t/\Delta x\approx0.03$) is needed for a stable solution. Figs. 7(a and b) show the plan and section views of the unsteady buoyant spreading at selected times. It is seen that the mixed jet fluid finds its level of density and spreads at the trapping level as a buoyant intrusion layer, with a weak counterflow both above and below; both the tracer concentration and velocity (not shown) profiles are relatively uniform within the layer. It is also noted that horizontal concentration gradients are negligible in the spreading layer; the layer thickness within $x=1-2Z_m$ is relatively constant as the front advances, where Z_m=maximum height of rise. The density intrusion displaces the surrounding fluid, and modifies the ambient density profile, resulting in increased density gradients both above and below the trapping level (Fig. 8). The ambient density is increased above the layer and decreased below it. Fig. 8(a) shows the predicted change in vertical salinity profile (at $x=1.24Z_m$ from source) is in excellent agreement with the experimental data. On the other hand, the alternative near-far field coupling methods fail to reproduce the observed change in ambient stratification. In particular, the thickness of the spreading layer is grossly underpredicted by AS and USTL approaches. For the DSTL method, the extra water introduced causes excessive reduction in the ambient salt concentration. Both the actual source (AS) and diluted source (DSTL) methods fail to reflect the change in ambient stratification even qualitatively. From the computed tracer distribution (of the 3D model), the minimum dilution can also be calculated from the predicted maximum concentration. Table 1 shows that the predicted dilution, trap level, and spreading layer thickness (defined by 0.1 $C_{\max}$ in the profile) are in good agreement with data, whereas the alternative predictions can dif-

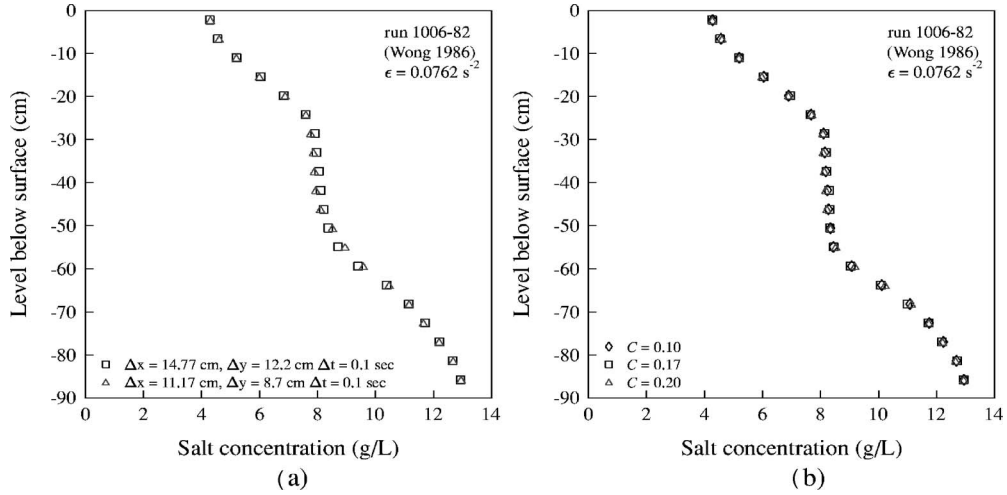

Fig. 9. Ambient salt concentration profiles before and after a round jet discharge into a linearly stratified fluid [observed data are adapted from Fig. 4.2.6 of Wong (1986)] for: (a) different horizontal grid sizes; (b) different horizontal diffusivities (C=dimensionless Smagorinsky parameter)

Table 1. Predicted Mixing and Spreading Layer Characteristics of a Vertical Round Buoyant Jet in Stagnant Linearly Stratified Ambient Fluid by Dynamic Coupling of Near- and Far-Field Models (DESA)

	Measured	JETLAG	Present method (DESA)	Actual Source (AS)	Diluted Source at Trapped Level (DSTL)	Undiluted Source at Trapped Level (USTL)
Minimum dilution at trapping level S_M	25.5	23.4	20.9	4.7	73.1	3.7
Maximum height of rise z_m	56	51.7	52.7	29.5	66.8	30.3
Level of minimum dilution in the spreading layer z_s	32	28.0	36.7	5.6	27.3	18.9
Spreading layer thickness h_s	20.5		27.1	25.1	74.2	16.1

fer greatly from the observations. It should be noted that in spite of the hydrostatic approximation, the jet overshoot or maximum height of rise can still be satisfactorily predicted. Sensitivity tests with different model grid sizes, horizontal and vertical eddy viscosities, and diffusivities have also confirmed the accuracy of the present model results (Fig. 9). It should be noted that the AS method does not simulate the near-field jet entrainment, and the DSTL method introduces excess flow and does not conserve mass.

Test Case 2: Turbulent Buoyant Convection from a Source in a Confined Region

Baines and Turner (1969) carried out laboratory experiments to study the effect of continuous convection from small sources of (negative) buoyancy on the properties of the environment when the region of interest is bounded. Fig. 10 shows a vertically sinking plume in an otherwise stagnant ambient fluid of initial uniform density ρ_a. The plume is discharged into a rectangular tank of length $L=57$ cm, width $W=45$ cm, and depth $H=45$ cm. Experiments have been carried out with a nozzle of diameter $D=5$ mm placed at $H=30$ or 40 cm above the bottom of the tank, with the initial level of fresh water about 0.5 cm above the discharge point. Different kinematic buoyancy flux $B_0=Q_0g\Delta\rho_0/\rho_a(0)$, where Q_0=discharge volume flux, were tested with an initial relative density difference $\Delta\rho_0/\rho_a(0)=0.13$. The buoyant plume mixes with the ambient fluid by turbulent entrainment; when it sinks to the bottom the mixed fluid spreads sideways as a bottom layer, with negligible vertical mixing (damped by density difference). The thickness of this layer of mixed fluid increases in depth with time, and the front of this bottom layer advances with a velocity dz/dt.

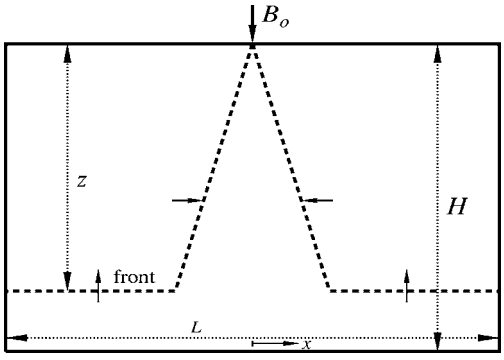

Fig. 10. Experiment of turbulent buoyant convection from a source in a confined region

A $19\times15\times20$ model grid closed at the four sides with horizontal grid size 3 cm by 3 cm and 20 uniform vertical layers and a time step $\Delta t=0.04$ s (with maximum $\mathrm{Cr}\approx2.66$) are used to simulate a round plume with buoyancy flux similar to those in the experiments. All simulations are cold-started. As shown in Fig. 11(a), the model predicts ambient density profiles that change from an initially uniform concentration to a stable stratification due to the action of the plume. It is interesting to note that for $t>12$ min, the ambient density profile is almost fixed in shape and changing at a uniform rate in time at all levels, with $d\rho/dt$ =constant—consistent with the self-similar asymptotic solution of Baines and Turner (1969). Fig. 11(b) shows that the predicted time variation of the interface (defined by 0.1 $\Delta\rho_{\max}$ contour, where $\Delta\rho_{\max}=(\rho_a)_{\max}-\rho_a(0)$, $z(t)$, is in excellent agreement with the following analytical solution [Eq. 6a of Baines and Turner (1969)] that is in excellent agreement with their experimental data:

$$\tau=5\left(\frac{5}{18}\right)^{1/3}[\zeta^{-2/3}-1] \tag{8}$$

in which $\zeta=z/H$ and

$$\tau=\frac{4}{\pi^{1/3}}\alpha^{4/3}\left(\frac{H}{R}\right)^2\frac{(B_0/2)^{1/3}}{H^{4/3}}t$$

with α=entrainment constant=0.1 and R=equivalent radius for the rectangular tank. In contrast, this interaction of the plume rise with the changing ambient condition cannot be satisfactorily simulated by either the AS method or the USTL methods.

Test Case 3: Inclined Plane Buoyant Jet in Stratified Fluid

The theory can be readily extended to treat two-dimensional situations. Lee and Cheung (1986) studied the mixing of a negatively buoyant slot jet in a linearly stratified fluid in a laboratory tank 3 m long, 0.328 m wide by 0.76 m deep (Fig. 12). A wooden partition was installed in the middle along the length of the tank to create an effective section with length of 6 m and width of 0.152 m. In addition to the maximum height of rise and the tracer concentration distribution in the spreading layer, the change in the ambient stratification caused by the jet discharge in the finite tank was also measured in the experiments (Lee and Cheung, private communication).

A $21\times3\times20$ model grid with closed boundaries at four sides is employed. The horizontal grid sizes are nonuniform in the y-

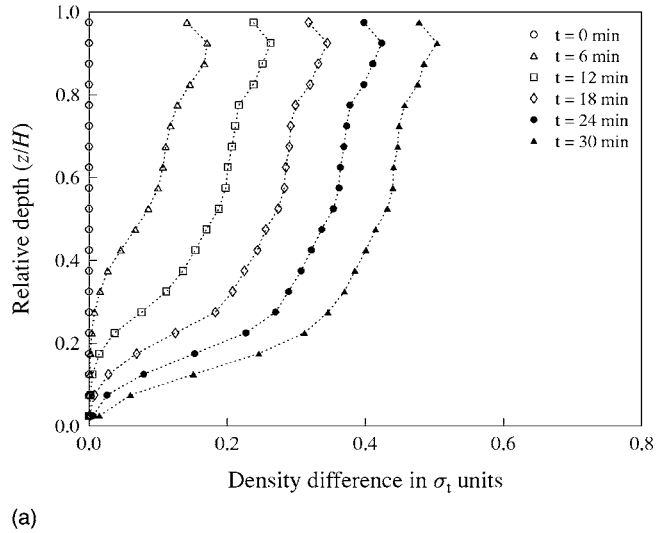

(a)

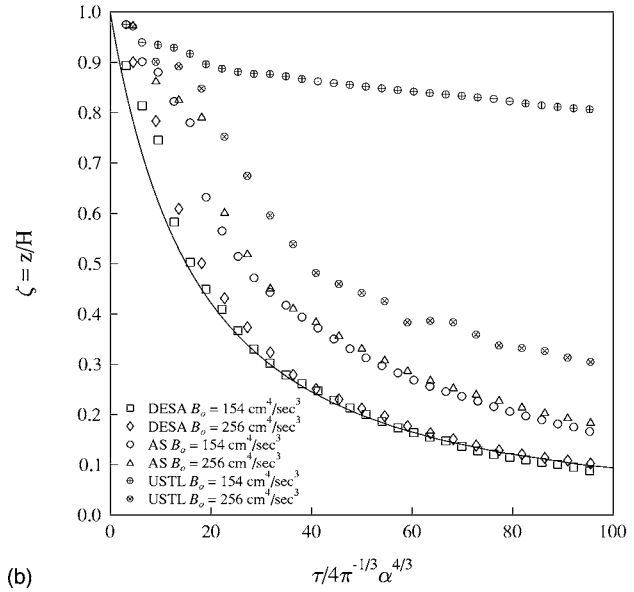

(b)

Fig. 11. (a) Predicted ambient density profiles at $x=5\Delta x$ from the jet at different times after release of a buoyant source with $B_0 = 154\ \text{cm}^4/\text{s}^3$; (b) computed time variation of dimensionless interface position (symbols) by different coupling methods. Solid line is best fit of experimental data represented by the analytical solution of Baines and Turner (1969) (given as Eq. 6a).

direction to account for the existence of the partition. The model is cold started with a time step of 0.05 s (with maximum Cr ≈ 0.88) and run for a duration of 5 min, similar to the length of experiment. Fig. 13(a) shows the numerical results for a vertical plane plume ($\theta_0=90°$) in linearly stratified fluid (Expt. P90-7 of Lee and Cheung). The initial volume, kinematic momentum, and buoyancy fluxes per unit length (Q_0, M_0, B_0) are 7.49 cm^2/s, 68.1 cm^3/s^2, and 49.5 cm^3/s^3, respectively, and the ambient stratification parameter is $\varepsilon=0.0855\ \text{s}^{-2}$. The plane (slot) jet can be represented by one or more noninterfering round jets with equivalent volume, momentum, and buoyancy fluxes per unit slot length. For the present case, it is found from the near-field model that the jet width of a single point source will cover the entire width of the tank at terminal level; it is hence sufficient to model the slot discharge by just one round jet. To assess the performance of such source representation, results with a 2D integral plane jet

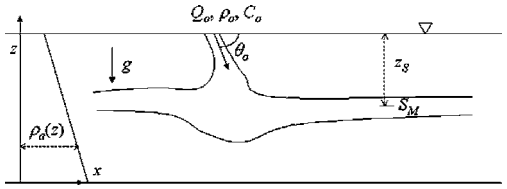

Fig. 12. Inclined plane negatively buoyant jet in linearly stratified fluid

model are also included for the purpose of comparison. Fig. 13(a) shows the predicted change in ambient density profile is in excellent agreement with the experimental data, whereas the other methods (not shown) distinctly fail in different aspects as in Test Case 1. It can also be seen that both the 2D jet and equivalent round jet source representation give similar results; the plane jet model performs slightly better especially for the region beyond "the maximum rise" level. Similar comparisons have also been obtained for jet-like and/or inclined discharges (not shown).

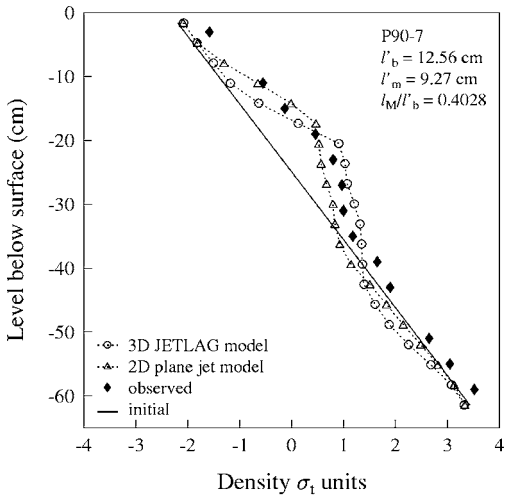

(a)

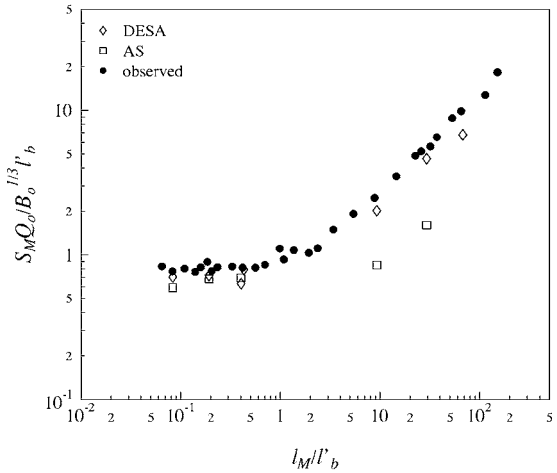

(b)

Fig. 13. (a) Ambient density profiles before and after a slot discharge into a linearly stratified fluid by DESA with different embedded near-field models; (b) comparison of computed and measured minimum dilution S_M in spreading layer for vertical plane buoyant jet in linearly stratified fluid

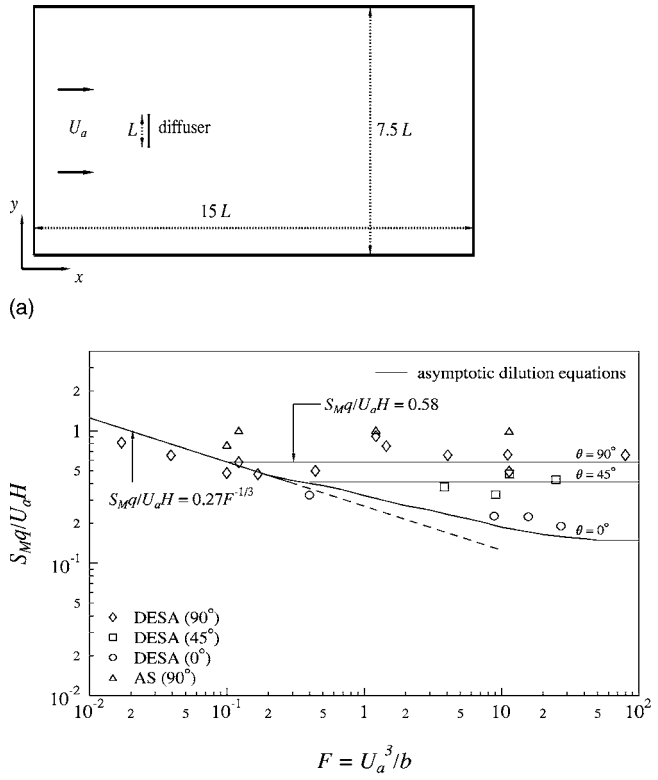

Fig. 14. (a) Experimental setup for finite line plume in a perpendicular cross flow; (b) computed minimum surface dilution as a function of cross flow Froude number F (symbols with coupling method indicated). Best fit of experimental data shown as asymptotic dilution equation (solid line).

Fig. 13(b) shows the predicted minimum dilution S_M in the spreading layer of a vertical plane buoyant jet with different initial momentum and buoyancy fluxes. The predicted dimensionless dilutions as a function of l_M/l_b', where $l_M=M_0/B_0^{2/3}$ and $l_b'=B_0^{1/3}/\varepsilon^{1/2}$ are in good agreement with the experimental data. The dimensionless minimum dilution is roughly a constant for "plume-like" discharge, $l_M/l_b'<1$, with a characteristic 2/3 power dependence for "jet-like" discharges, $l_M/l_b'\gg 1$. As a comparison, the AS method generally predicts lower plume trapping levels and hence lower dilution S_M.

It should be pointed out that, in all the previous three cases, due to the introduction of the discharge, the water depth is gradually changing during the experiment. The change in depth is fully catered for by the circulation model. In all cases the mixing in the intermediate field—resulting from the coupling of the near-field vertical plume rise and the horizontal gravitational spreading layer—is well predicted.

Test Case 4: Line Plume in Perpendicular Cross Flow

Finally, the DESA method is demonstrated for the practically important problem of a finite "line plume" in a cross flow. Roberts (1979) performed experiments in a 6.1 m wide by 11.0 m long rectangular basin with a slot diffuser discharge in a steady current [Fig. 14(a)]. Experiments were carried out for a wide range of current speed U_a and discharge buoyancy flux b per unit length. The experiments show that the near-field dilution is governed by a cross flow Froude number, $\mathsf{F}=U_a^3/b$, representing the ratio of ambient velocity to buoyancy-induced velocity. Small values of F indicate a buoyancy-dominated flow, resulting in the formation of a buoyant surface wedge with an initial width greater than the diffuser length. On the other hand, high values of F represent a flow dominated by the ambient current. For this case, a $23\times 17\times 20$ model grid with open boundaries at two ends, a horizontal grid size of 43.5 cm by 30.5 cm, and 20 uniform vertical layers is employed. The model is run to generate a steady state current field first before the line plume is applied and the time step ranges from 0.01 to 0.05 s (with maximum $\mathsf{Cr}\approx 0.10$). The finite line plume of length $L=0.61$ m is represented by a number (n) of equivalent noninterfering round plumes (preserving the same volume, momentum, and buoyancy fluxes per unit diffuser length). The number can be determined from the jet simulations, and $n=4-6$ are required for the present case. In addition, similar results are obtained with the ambient concentrations computed by (1) averaging values in all the surrounding cells as indicated in Fig. 4(c); and (2) averaging only those in the "upwind" cells. Fig. 14(b) shows the predicted dimensionless minimum surface dilution $S_M q/U_a H$ (inferred from the maximum concentrations in the surface layer) for three diffuser orientations to the current: $\theta=90°$ (perpendicular alignment), 45°, and 0°. It can be seen that the predicted dilution [computed using averaging method (1)] agrees well with the asymptotic dilution equation (best fit of data) given by Roberts (1979), where $q=Q_0/L$=unit discharge. On the other hand, the actual source method (for the perpendicular alignment) is seen to overpredict initial dilution. In Fig. 15(a), the observed surface waste-field pattern is compared with the predicted surface concentration contours for three representative flow situations, with $\mathsf{F}\approx 0.13$, 1.3, and 11.4 [corresponding, respectively, to Experiments H5, H4, and H3 in Roberts (1979)]. Fig. 15(b) shows the corresponding computed concentration field in a vertical section in the centerline plane of symmetry. The DESA predictions are very similar to the experimental observations: (1) With $\mathsf{F}\sim 0.1$, the mixed effluent has a plume-like pattern, with a surface buoyant layer and significant lateral spread. The surface width at the diffuser is larger than the diffuser length; both the extent of the upstream intrusion and the lateral width are well supported by the observations. (2) As F increases, the surface buoyant layer is swept downstream; the lower surface concentrations for $\mathsf{F}\geqslant 1$ indicates bottom attachment of the effluent field. (3) For $\mathsf{F}\sim 10$ the flow is advection-dominated and the lateral spread of the surface field is very limited. Overall, the predicted flow features agree well with the observations in Roberts (1979); the computed length of bottom attachment is also broadly similar to the reported values. The predicted shape of surface field by the AS method is similar to that of DESA; however the AS method cannot reproduce the buoyant layer close to the near field. In Fig. 16, the normalized vertical profile of tracer concentration along the centerline, CU_aH/q, is compared with data at different downstream locations. It can be seen that the DESA method predicts the tracer concentration field in the spreading layer quite well, whereas the AS method tends to predict exaggerated vertical mixing.

Test Case 5: Line Plume in Stratified Cross Flow

Roberts et al. (1989) conducted experiments in a stratified towing tank 1.2 m deep, 2.4 m wide, and 25.0 m long. A nominal buoyancy frequency

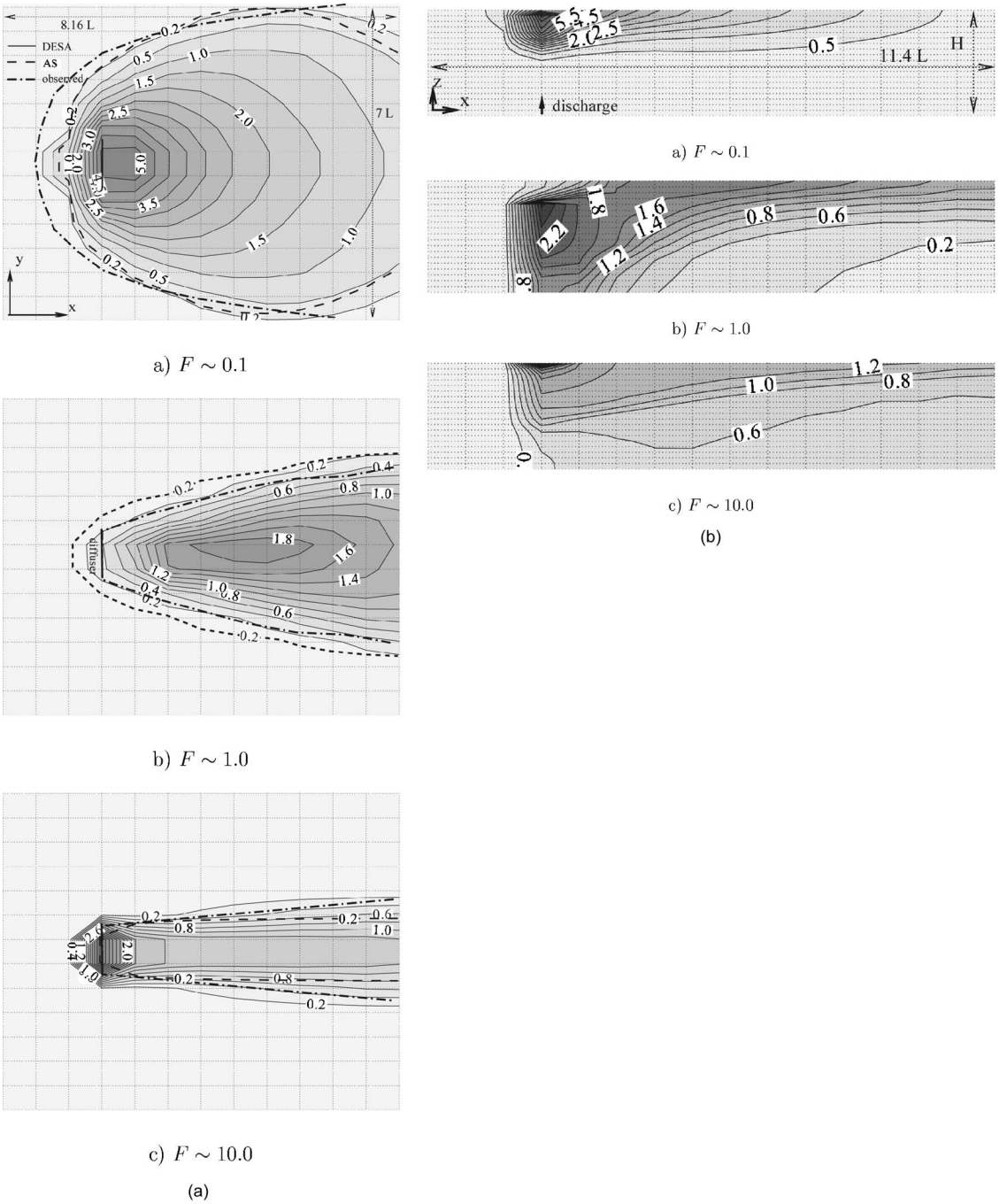

Fig. 15. (a) Computed surface tracer concentration field (in units of $0.01C_0$) and observed surface field for a finite line plume in a perpendicular cross flow; (b) Computed tracer concentration field for a vertical section in the plane of symmetry for finite line plume in a perpendicular cross flow (concentration in $0.01C_0$).

$$N = \sqrt{-\frac{g}{\rho_0}\frac{d\rho}{dz}}$$

of 0.3 s^{-1} and a multiport diffuser of length $L=1.2$ m were used in all experiments. For this case, a $41\times8\times20$ model grid with open boundaries at two ends, a horizontal grid size of 60.0 cm by 30.0 cm, and 20 uniform vertical layers is employed. The model is run to generate a steady state current field first before the line plume is applied and the time step used is 0.025 s (with Cr ≈0.29). Fig. 17 shows the predicted minimum dilution (maximum concentration in spreading layer) and level of minimum dilution. The calculations show that the AS method predicts exaggerated mixing, and hence a much lower trapping level than that predicted by the DESA method. For the cases with $\mathrm{F}=U_a^3/b\geqslant 1$, the simulated plumes (by AS) remain in more or less the same (source) level. Roberts et al. (1989) reported for $\mathrm{F}\approx0.1$, the rise height (the level of minimum dilution), z_s, is about $2l_b$ and follows an inverse 1/6 power law for $\mathrm{F}\geqslant5$ given by: $z_s/l_b=1.5\mathrm{F}^{-1/6}$ where $l_b=b^{1/3}/N$. As shown in Fig. 17, the plume trapping level predicted by DESA agrees well with the above-presented equation. The minimum dilution data at the plume trapping level can also be described by: $S_M qN/b^{2/3}=2.19\mathrm{F}^{1/6}-0.52$ for the range $0.1<\mathrm{F}<100$. Again the computed dilution by

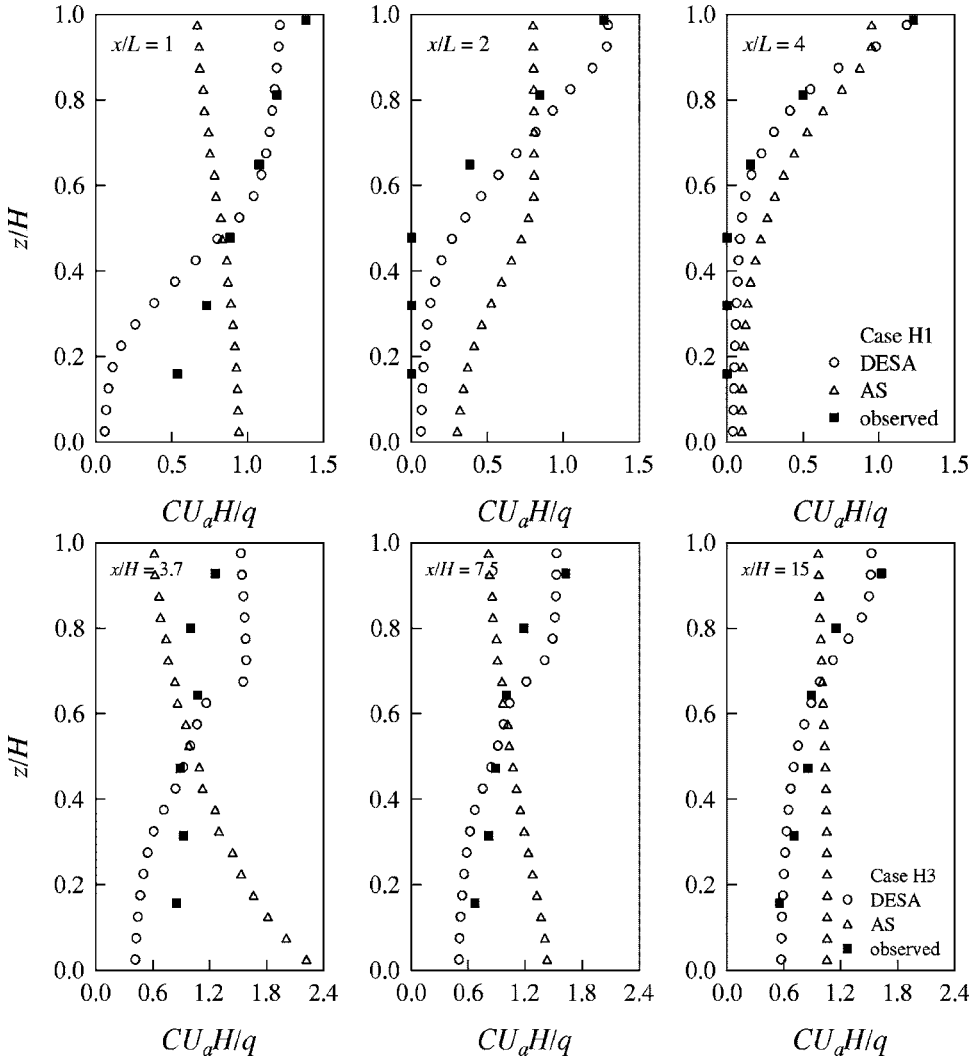

Fig. 16. Normalized vertical profiles of tracer concentration (C) along centerline for perpendicular flow alignment, for F=1.26 (Case H1) and F=11.8 (Case H3 in Roberts 1979). Observed data are adapted from Fig. 5.13 and 5.14 of Roberts (1979).

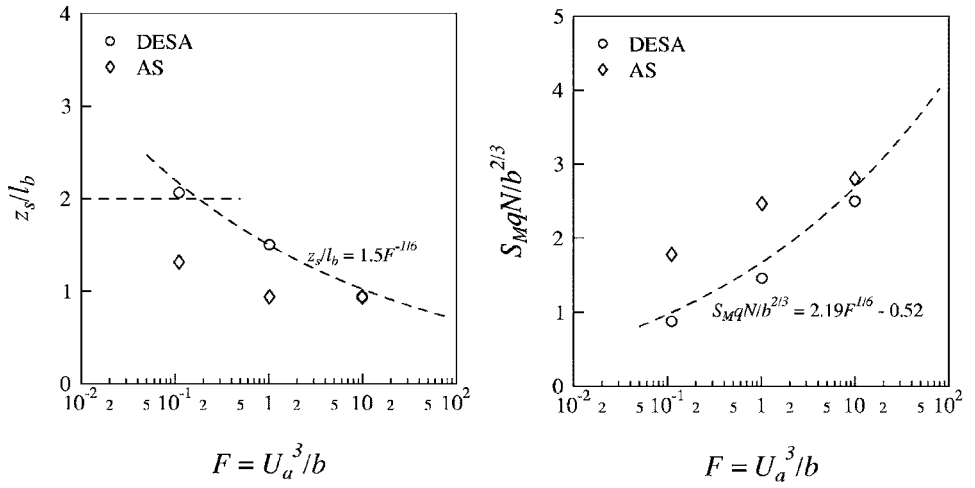

Fig. 17. Predicted level of minimum dilution z_s and minimum dilution S_M (symbols) for line plume in stratified cross flow

DESA compares well with this equation, while the AS method overpredicts the dilution especially for smaller F.

Concluding Remarks

Effluent mixing in the near to intermediate/far field has been successfully modeled by a new method of coupling plume models with 3D circulation models. In many practical situations the near-field mixing can be well predicted by integral jet models based on the boundary layer approximation. By representing the jet as a system of distributed entrainment sinks and diluted source at terminal level, the effect of near-field plume mixing can be well represented in a 3D circulation model based on the hydrostatic approximation. A true dynamic coupling between the plume rise in the near field and the gravitational spreading in the intermediate field is achieved along with full water and tracer mass (buoyancy) conservation. The use of the proposed Distributed Entrainment Sink Approach (DESA) effectively captures the physics of plume mixing as predicted by a subgrid integral jet model. The DESA method is generally applicable to both laboratory and prototype flow situations. Tests for a variety of complex flow scenarios have confirmed that numerical predictions are in excellent agreement with experimental data—without the need to use non-hydrostatic circulation models to resolve the plume mixing, or *ad hoc* adjustment of far-field model mixing coefficients. Extensive numerical experimentation has shown that the method can be applied using horizontal grid sizes in the range of $0.5H-3H$ for the intermediate field close to the source, and 15–20 uniform layers to resolve the vertical structure. The general and robust method can be readily implemented in existing circulation models to yield accurate predictions of the intermediate/far field for many environmental transport problems. An example of the application of DESA for prototype tidal flows and pollution discharges can be downloaded from the VISJET Web site (http://www.aoe-water.hku.hk/visjet).

Acknowledgments

The work reported herein is supported by a grant from the University Grants Committee of the Hong Kong Special Administrative Region, China (Project No. AoE/P-04/04) to the Area of Excellence (AoE) in Marine Environment Research and Innovative Technology (MERIT).

References

Baines, W. D., and Turner, J. S. (1969). "Turbulent buoyant convection from a source in a confined region." *J. Fluid Mech.*, 37, 51–80.

Bleninger, T., and Jirka, G. H. (2004). "Near- and far-field model coupling methodology for wastewater discharges." *Environmental hydraulics and sustainable water management*, J. H. W. Lee and K. M. Lam, eds., Taylor & Francis, London, 447–453.

Blumberg, A. F., Ji, Z. G., and Ziegler, C. K. (1996). "Modeling outfall plume behavior using far field circulation model." *J. Hydraul. Eng.*, 122(11), 610–616.

Choi, K. W. (2002). "Environmental management of mariculture in Hong Kong." Ph.D. thesis, The Univ. of Hong Kong, Hong Kong.

Hamrick, J. M. (1992). "A three-dimensional environmental fluid dynamics computer code: Theoretical and computational aspects." *Special Rep. No. 317*, The College of William and Mary, Virginia Institute of Marine Science.

Hamrick, J. M. (1996). "User's manual for the environmental fluid dynamics computer code: Theoretical and computational aspects." *Special Rep. No. 331*, The College of William and Mary, Virginia Institute of Marine Science.

Jirka, G. H., and Lee, J. H. W. (1994). "Waste disposal in the ocean." *Water quality and its control, IAHR design guide for hydraulic structures*, Balkema, Rotterdam, The Netherlands, 193–242.

Kim, Y. D., Seo, I. W., Kang, S. W., and Oh, B. C. (2002). "Jet integral-particle tracking hybrid model for single buoyant jets." *J. Hydraul. Eng.*, 128(8), 753–760.

Koh, R. C. Y. (1983). "Wastewater field thickness and initial dilution." *J. Hydraul. Eng.*, 109(9), 1232–1240.

Lee, J. H. W., and Cheung, V. (1986). "Inclined plane buoyant jet in stratified fluid." *J. Hydraul. Eng.*, 112(7), 580–589.

Lee, J. H. W., and Cheung, V. (1990). "Generalized Lagrangian model for buoyant jets in current." *J. Environ. Eng.*, 116(6), 1085–1106.

Lee, J. H. W., and Chu, V. (2003). *Turbulent jets and plumes—A Lagrangian approach*, Kluwer Academic, Dordrecht.

Mellor, G. L., and Yamada, T. (1982). "Development of a turbulence closure model for geophysical fluid problems." *Rev. Geophys. Space Phys.*, 20(4), 851–875.

Roberts, P. J. W. (1979). "Line plume and ocean outfall dispersion." *J. Hydr. Div.*, 105(4), 313–331.

Roberts, P. J. W., Snyder, W. H., and Baumgartner, D. J. (1989). "Ocean outfalls. I. Submerged wastefield formation." *J. Hydraul. Eng.*, 115(1), 1–25.

Thatcher, M. L., and Harleman, D. R. F. (1972). "A mathematical model for the prediction of unsteady salinity intrusion in estuaries." *Rep. No. 144*, Ralph M. Parsons Laboratory for Water Resources and Hydrodynamics, Dept. of Civil Engineering, Massachusetts Institute of Technology, Cambridge, Mass.

Turner, J. S. (1973). *Buoyancy effects in fluids*, Cambridge University Press, Cambridge, Mass.

Wallace, R. B., and Wright, S. J. (1984). "Spreading layer of a two-dimensional buoyant jet." *J. Hydraul. Eng.*, 110(6), 813–828.

Wong, D. R. (1986). "Buoyant jet entrainment in stratified fluids." *Rep. No. UMCE 85-9*, The Univ. of Michigan.

Zhang, X. Y., and Adams, E. E. (1999). "Prediction of near field plume characteristics using far field circulation model." *J. Hydraul. Eng.*, 125(3), 233–241.